れるようになり，ますます薬物療法の担う重要度は非常に高くなってきた．また，外来化学療法システムの構築により，これらの化学療法が，入院治療から外来通院型治療への移行も進んでいる．点滴抗癌剤治療に共通な副作用に骨髄抑制（白血球減少が中心）があり，ときに発熱などの臨床症状に遭遇する．好中球減少に伴う感染症は，不適切な治療の場合，急激に進展し，死に至ることも少なくないので，発熱性好中球減少症に対するマネージメントは非常に重要である．

1．発熱性好中球減少症の定義

2003年に公表されたRecommendations for antimicrobial use in febrile neutropenia in Japan[1]が最新のガイドラインであるが，ここでは発熱性好中球減少症とは，①発熱：1回の検温で腋窩≧37.5℃または口腔内≧38℃，②好中球：好中球数が500/mm³未満，または1,000/mm³で500/mm³未満に減少することが予測される場合と定義されている．

2．歴史的背景

悪性腫瘍の化学療法中に経験される発熱症例の約半数は，血液培養が陰性で不明熱とされることが多かったが，その中でも多くの症例で抗菌薬が奏効すること，一方敗血症に進展する症例もあることから，感染症と認識され，1990年にKlasterskyらはこれらの病態も含めて，Febrile Neutropenia（FN）と命名した．米国感染症学会は1990年にガイドラインを発表し，2002年に最新の改訂を行った[2]．わが国では，1998年に宮崎コンセンサスが発表されたが，改訂を加え，FNガイドライン2003[1]が作成された．本稿ではこのガイドラインに従いつつ，乳癌治療の実地臨床に沿ったFN対策を紹介したい．

3．乳癌化学療法の実際

近年の乳癌化学療法において汎用される標準的レジメは，アンスラサイクリン系薬剤含有レジメとタキサン系レジメであろう．アンスラサイクリン系レジメとしては，AC療法（A：Adriacin® 60 mg/m²，C：cyclophosphamide 600 mg/m²，3週間隔）やCEF療法（C：cyclophosphamide 500～600 mg/m²，E：epirubicin 75～100 mg/m²，F：5-FU 500 mg/m²，3週間隔）が代表的である．また，タキサン系レジメとしては，Paclitaxel(175～210 mg/m²，3週間隔，もしくは80 mg/m²，1週間隔)やDocetaxel 60～75 mg/m²，3週間隔の投与方法が広く行われている．これらの薬剤による好中球減少の時期（Nadir）は，宿主の状態（年齢，PS，栄養状態，遺伝的要素など）にも影響され，個人差はあるものの，各薬剤におおよそ時期が決まっている．乳癌の標準的治療で使用される上記の薬剤のNadirは7～14日目で，回復時期は14～21日とされている．つまり，後述のように，このNadirの時期を中心に適切なケア（予防）と，FN発症時の適切な診断と治療が重要である．

4．発熱性好中球減少症の診断とリスク分類

経過観察中に発熱を認めたら，検血(白血球分画)，一般生化学検査，CRP，胸部X線検査，血液培養検査などを行い，病態の把握と起炎菌の同定を進める．FN患者のリスク分類が提唱されており，Klasterskyらによる予測モデル[3]では，**表1**に示すスコアリングインデックスにより，合計が21点以上では低リスク，20点以下では高リスクで重症化する可能性がある．リスクに応じた治療方法が推奨されている．MDACCではさらに簡略化し，①外来患者②標準的治療を受けている固形腫瘍③好中球減少が7日以内

表1　発熱時のリスク判定用スコアリング

臨床症状	なし：軽度：5　中等度：3
低血圧	なし：5
慢性閉塞性肺疾患	なし：4
固形腫瘍で真菌感染	なし：4
脱水症状	なし：3
発熱時外来管理	yes：3
60歳未満	yes：2

※点数の合計が21点以上が低リスク群

表2　CTCAE ver3.0 (Common Terminology Criteria for Adverse Events)にみる発熱性好中球減少に関連する事象

Grade	1	2	3	4	5
白血球（/mm³）	<LLN～3,000	<3,000～2,000	<2,000～1,000	<1,000	死亡
好中球/顆粒球（/mm³）	<LLN～1,500	<1,500～1,000	<1,000～500	<500	
発熱（Grade 3以上の好中球減少を認めず）	38～39°C	>39～40°C	>40°C以上が24時間以内	>40°C以上が24時間以上	
発熱性好中球減少（Grade 3～4の好中球減少を伴う感染で感染巣不明）			あり	生命を脅かす（敗血症ショック・血圧低下・アシドーシスなど）	
Grade 3～4の好中球減少を伴う感染(臨床的に確認)		限局性・局所的処置を要する	抗生物質の静脈投与・抗真菌薬・抗ウイルス薬の投与や外科的処置を要する		
Grade 0～2の好中球減少を伴う感染					
好中球数不明の感染					
口内炎	粘膜の紅斑	斑状潰瘍または偽膜	癒合した潰瘍または偽膜，わずかな外傷で出血	組織の壊死，著明な自然出血，生命を脅かす	

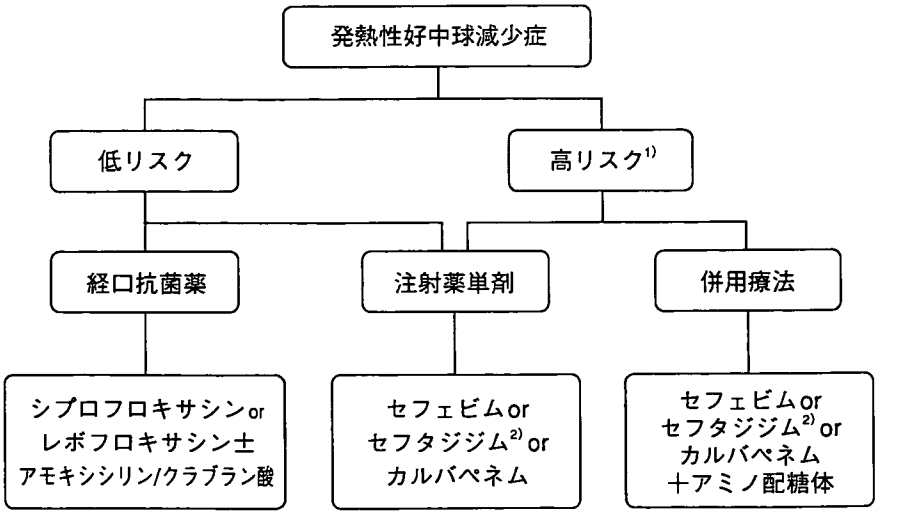

図1　初期治療方針

3～5日後に再評価を行う．
1）MRSA（メチシリン耐性黄色ブドウ球菌）が検出されたらグリコペプチド（バンコマイシンなど）を追加
2）セフタジジム耐性のグラム陽性菌，グラム陰性菌が増えている．

④合併症がない場合は低リスク患者としている[4]．乳癌患者の多くは初期発見時には多くは低リスクに該当する．しかし，いずれにせよ，治療開始が1日でも遅れた場合には死亡率が高くなることは周知の事実であり，起炎菌の培養などの同定結果を待つのではなく，発症と同時に治療の開始が必要である．

また，諸報告によるとFNの場合，40～90%と高率で起炎菌が同定できないことから，各時代および各施設における感染症の起炎菌の変遷も理解しておく必要もある[5]．起炎菌の確定には好中球に貪食された菌のDNAを同定する検査法として，白血球細菌核酸同定法（in situ hybridization；ISH）の実地応用も進んでいる[6]．

化学療法中の有害事象の記載には，CTCAE ver3.0 (Common Terminology Criteria for Adverse Events)[7]に従ったGrade評価で共通の手法で記載する必要がある（**表2**）．定義に基づくFNの出現は，Grade3と評価される．

5．ガイドラインに準拠した初期治療

わが国のガイドラインに示された初期治療のアルゴリズムを**図1**に示す[1]．

1) 低リスク群

キノロンが原則で，経口抗生物質のシプロフロキサシン（CPFX），レボフロキサシン（LVFX）を使用する．口内炎などの病変があるときには，グラム陽性球菌に対して有効なアモキシシリン/クラブラン酸(AMPC/CVA)，セファロスポリンなどの併用が勧められる．また必要に応じて，注射剤の単剤投与も選択される．

2) 高リスク群

まずMRSA（メチシリン耐性黄色ブドウ球菌）の感染があるか否か，つまりバンコマイシン（VCM）の適応があるかどうか判断する．通常は，第4代セフェム（セフェピム：CFPM)，セフタジジム，カルバペネムの単剤投与が選択されるが，最近，セフタジジムには耐性菌が増加しており，これらのempiric therapyには勧められない．重症化・遷延化が予測される場合はアミノグルコシドとCFPMあるいはカルバペネムを併用することが推奨される．VCMの必要な高リスク患者には，VCM±アミノグルコシドとCFPMあるいはカルバペネムを併用する．

CFPM（マキシピーム®）は発熱性好中球減少症に対して米国で唯一FDAに承認された薬剤で，わが国でも2004年9月にFNに対する効能・効果が追加承認された．現在，FNの適応を有する抗生物質は本剤のみである．通常感染症の場合には，1日1～2g(力価)を2回に分割し，静脈内注射もしくは点滴静注するが，FNに対しては，1日4g（力価）を2回に分割投与する方法が認可されている．投与期間は原則14日までとされるが，乳癌患者の多くでは長期間必要とする例はまれである．

わが国におけるFNガイドライン2003の妥当性および単剤法か併用法かに関してはFN一次研究（2000．5～2002．2）のデータが公表されている[8,9]．FN患者に対して，セフェピム（CFPM）単独投与とセフェピム＋アミカシン(CFPM＋AMK)併用法の比較試験であるが，3日目にそれぞれ33%，46%で著効が認められ，7日目には51%，59%と有意な差は認められなかった．しかし，3日目で好中球数が500/mm^{3}未満の症例では併用群で有意に有効率が高かった（46% vs 28%；p=0.024）ことから高リスク群には併用が勧められる．

6．初期治療開始後のfollow

治療開始後の3～5日に初期治療の評価を行う．

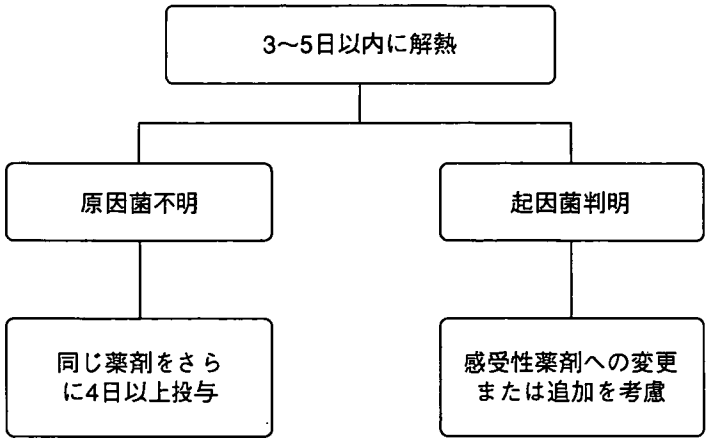

図2　治療開始3～5日以内に解熱した場合のfollow

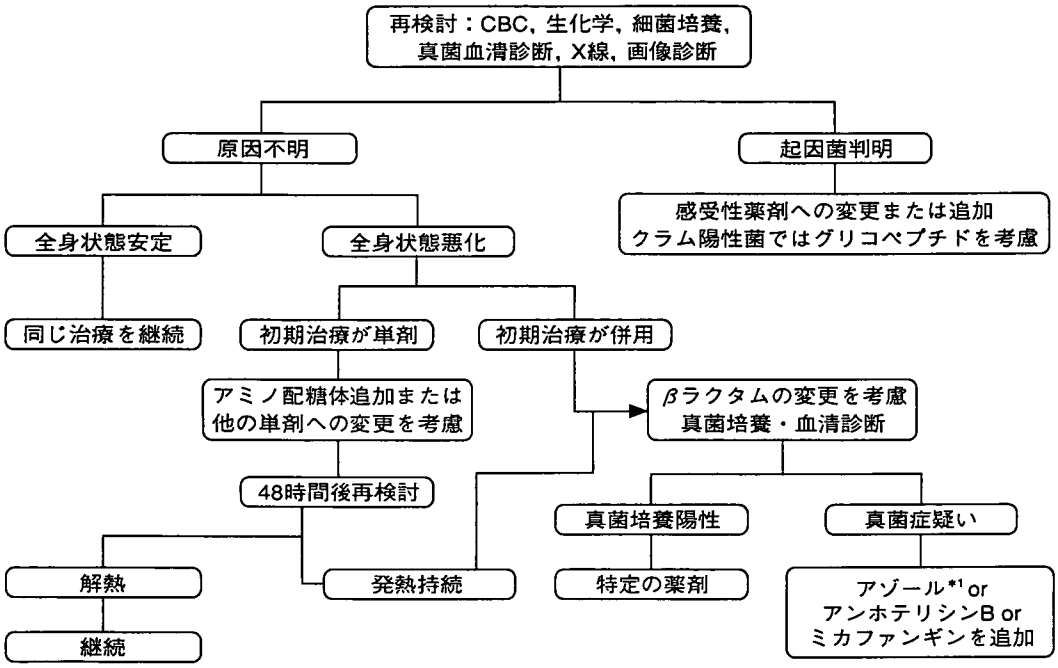

図3　治療開始後3～5日後も解熱しない場合の治療方針
GCSFやガンマグロブリンを投与していない場合は追加を考慮する．
*1 予防投与されていない場合のみ

1) 初期治療が奏効した場合（図2）

原因菌が同定できれば，その感受性薬剤への変更や追加も考慮される．原因菌不明な場合は，初期治療と同じ薬剤を継続する．解熱しても，初期治療から7日間の抗生物質の投与が勧められるが，好中球数が500/mm³以上に回復したら，抗菌剤の投与は終了する．

2) 初期治療が奏効しない場合（図3）

患者の臨床状態が安定していたら，初期治療と同じ内容を継続してもよいが，最初に単剤投与を行った場合には，アミノ配糖体薬剤の追加もしくは他の薬剤への変更も考慮することが実際には多い．アミノグルコシドの併用は相乗効果が得られ，かつ耐性菌の出現を増加させないメリットがあると考えられている．

5日以上発熱が持続する場合は，カンジダやアスペルギウス，フサリウムなどの真菌感染症，ウイルス感染症などを疑って，アンホテリシンBなどの抗真菌剤の投与開始を考慮する．

3) G-CSF (granulocyte colony stimulating factor)・ガンマグロブリン

G-CSFや顆粒球輸注，ガンマグロブリンをルーチンで使用することは，ガイドラインでは推奨されない[1,2]．特に低リスクで好中球が1週間で回復すると予測される場合，G-CSFの使用は不要である．重度の感染症や初期治療に奏効しない場合は，G-CSFの投与も考慮する．G-CSFの使用ガイドラインに関しては，2001年に癌治療学会から公表されている[10]．基本的にはわが国の保険制度遵守(化学療法による好中球減少症で好中球1,000/mm³未満で38°C以上の発熱，または好中球500/mm³未満）が必要であるが，無熱の場合は，この使用を強く勧めるエビデンスに乏しく差し控えるべきである．

G-CSFとして使用できる薬剤は，わが国では，filgrastin（グラン®），lenograstin（ノイトロジン®），nartograstin（ノイアップ®）の3種類が挙げられる．いずれの薬剤でも効果に大差はないようである．癌種や宿主の状態により用法用量が異なるので注意が必要である．実際には，乳癌化学療法時に使用する用量の基準は，グラン®（50μg/m²皮下注），ノイトロジン®（2μg/kg皮下注），ノイアップ®（1μg/kg皮下注）である．

ガンマグロブリンの使用については，FNが遷延する場合や重症化が予測されるときには抗生物質との併用でその使用を考慮することも必要である．

7．発熱性好中球減少症（FN）の臨床像

1) 好中球数と感染のリスク

好中球数（Absolute neutrophil count：ANC）は，白血球数×［segs (segemented neutrophils) %＋bands (young neutrophils)］で計算される．

1,500/mm³以上では感染のリスクはなく，1,000～1,499でslight, 500～999でmoderate, ＜500でhigh riskとされる．多くの実地臨床や臨床試験において，化学療法の開始基準に好中球数1,500/mm³以上とされる根拠でもある．

2) 好中球減少症（Neutropenia）の原因

化学療法のレジメ，用量・用法，他の併用療法，留置カテーテルの有無などの治療側因子と，年齢，栄養状態，癌種，癌のステージなどの宿主側因子の関与が考えれる．FNのリスク予測と予防に関してはこれらの因子の関わりを考え，患者指導が大切である．

3) FNの臨床症状

NCCNが2002年に公表した"Fever and neutropenia：treatment guidelines for patients with cancer"[2]を参考にすると，**表3**に示すような症状が出現時には感染を疑うことを，患者説明用パンフレットに示されている．該当する症状があれば，4回以上の熱の測定，38°C以上で受診，熱形表の記載，水分補給(水やフルーツジュース)，十分な休養，保温，前頭部の冷庵などの対応をとるように指導されている．

4) 感染の分類

前述のように，FNの起炎菌が確定されることは，全体の半数以下であるが，培養同定できた菌のスペクトルは，時代とともに変遷している．わが国の血液疾患を扱う施設でのデータではあるが，1985年から1996年には，グラム陽性菌の頻度が高かったが，1997年から2000年にはグラム陰性菌が主体となった．しかし，この菌のスペクトルには各施設の一般病室の菌叢分布や抗生剤の予防投与の有無にも影響を受け，特に積極的に予防投与を行っている施設ではグラム陽性菌の方が頻度が高いとの報告もある．薬剤耐性も問題で，近年では緑膿菌の30%がイミペネム，22%がセフピローム，15%がピペラシリン，12%がセフェピムおよびセフタジジムに耐性を示している[5,11]．

適切な抗生物質の投与にも関わらず，高熱が続く場合は，真菌症を疑い，早期の対策が重要で，実際

表3　発熱性好中球減少症の初期臨床（文献2）を改編）

皮膚温の上昇
倦怠感
体の痛み
ふるえ・悪寒
咳・息切れ
排尿時の痛み
嚥下時の違和感
咽頭痛
口腔内のただれ・痛み
鼻汁・鼻閉感
イライラ感
めまい
頭痛
外傷・手術・点滴部位の発赤・腫脹・熱感
腹痛
下痢
直腸の不快感

患者のこのような症状が出ると熱を測定するように指導したい

表4　好中球減少時の自己ケアのポイント（文献2）を改編）

大衆の中や感冒・感染症の有する人との接触をさける
体の清潔を維持
手洗い（入浴後，食事前，外出後）
口腔内ケア（歯磨き・うがいなど）
便秘を避ける（緩下剤の使用）
運動や水分補給で腸管運動を維持
部屋に生花や植物の設置を避ける
ペットの糞尿を避ける
食器などの洗浄には加熱水を使用
バスタオルやグラスは他人のものを共用しない
食べてはいけないもの・飲んではいけないもの
低温滅菌されていないミルク
チーズやヨーグルト
生肉・生魚・生卵・豆腐
チーズベースの味付けサラダ
生野菜・フルーツ
低温滅菌されていないフルーツ・野菜ジュース
低温滅菌されていないビール

に乳癌の標準的な抗癌剤治療を受ける患者の中にも難渋するFNで抗真菌剤が奏効したケースも経験する．

ときにFN発現の時期に前後して，帯状疱疹ヘルペスなどのウイルス疾患も合併することも経験する．抗ウイルス剤の投与とともに，FN発症のリスクを念頭におき，経過を十分に観察することが重要である．

5) FNの予防

NCCNガイドラインから，好中球減少期間の予防策を**表4**に示す．FNを理解し，適切な対策を十分に理解してもらうことが，外来通院型化学療法とクール間の外来通院省略の普及には必須である．FNを適切にマネージメントすることが，われわれ医療従事者にとってチーム医療の機能評価としての重要な項目である．

8．国立病院機構大阪医療センターにおけるFN対策の実際

1) 患者説明とFN対策指導

当院では再発でPSの悪い患者以外は，全例標準的化学療法は外来通院でスタートし，クール間の外来受診は，何か困った予期せぬ症状があった場合の緊急受診を除いて，基本的には勧めていない．このシステムを可能にしたのは，チーム医療を中心としたシステムの整備や患者指導（セルフケア指導）の統一などが挙げられる．

FNについては，まず担当医が治療方法の説明と同時に，治療中の白血球数の変動と易感染性状態，その対策を説明する．その際には，単にすでに記載されたパンフレットを手渡すのではなく，口頭での説明と同時に患者の反応から理解度を把握し，その場で図示と記録を行い，それを手渡すようにしている（**図4**）．手書きではあるが，患者の理解を促しながら個人個人の必要度に応じた説明ができる利点がある．具体的には，Nadir時期を中心とした手洗いやうがい，口腔内ケアによる予防と，発熱時対策として，38°C以上の発熱を認めた場合には，あらかじめ処方したシプロキサン1,200 mgを分3で3日間内服してもらう．3日間内服しても解熱しないとき，また経過中に39°C以上の発熱があれば，いつでも救急受診をするように指導する（**図5**）．口内炎がFNの引き金になることもあるので，出現時にはazulene（ハチアズレ®）を用いた含嗽を勧めている．これらの説明を担当医師，外来化学療法室専任看護師や薬剤師

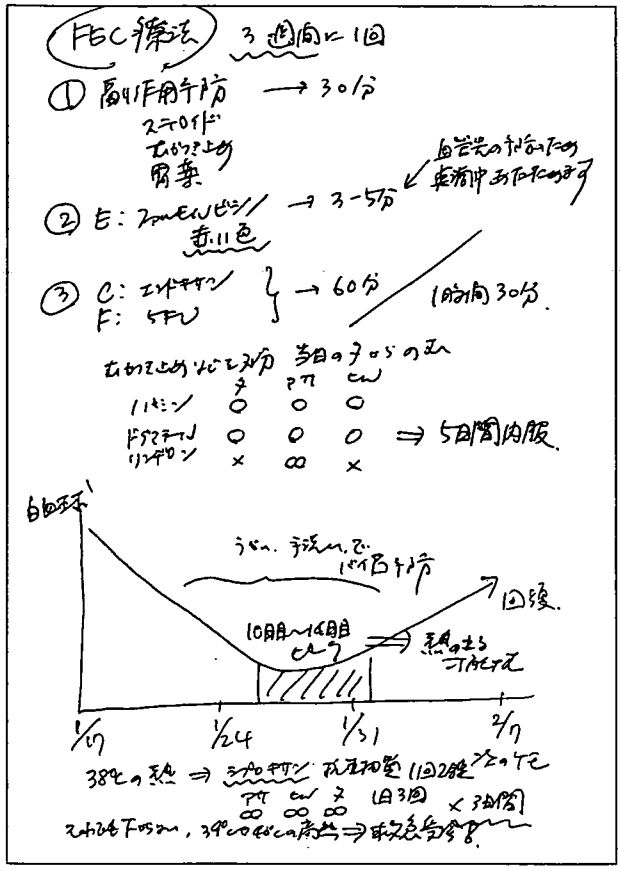

図4　FEC療法開始時の説明メモ1例
口頭説明しながらポイントを同時にメモに記し，患者に手渡すことで理解度を上げる工夫．

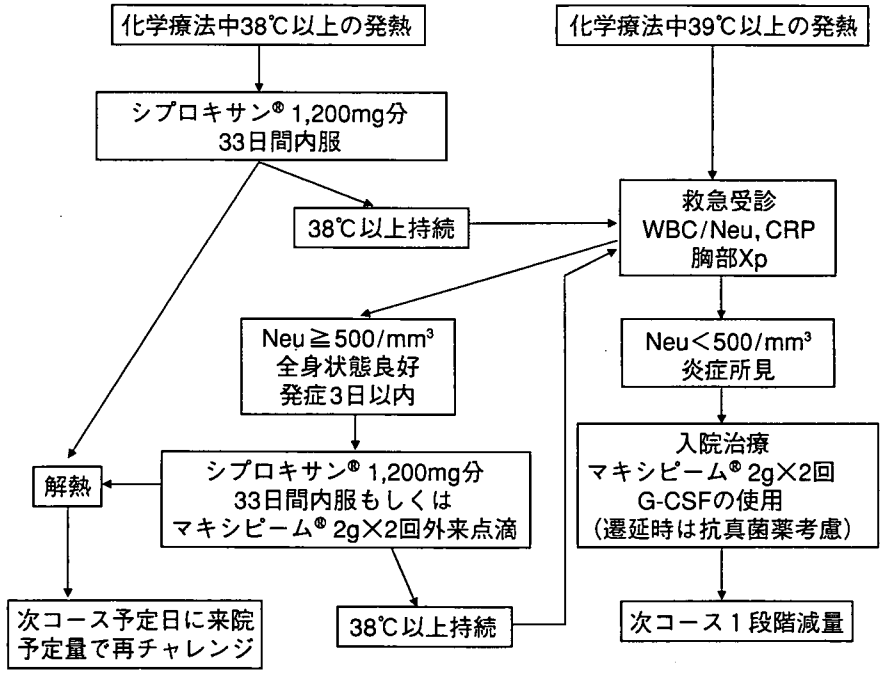

図5　国立病院機構大阪医療センターにおけるFN治療方針

から2回3回と繰り返し説明を受けることにより，患者の理解を高める工夫を行っている．また，次に示す標準的レジメでは，これらの対策内容を統一することで，医療従事者からの指導のみならず，患者間での情報交換による支えあいも有効に利用できる環境になっている．

2) 乳癌標準的化学療法におけるFNの頻度

当院では標準的化学療法のレジメとして，アンスラサイクリン系レジメはFEC（C：cyclophos-

phamide 500～600 mg/m², E：eripubicin 75～100 mg/m², F：5-FU 500 mg/m², 3週間隔), タキサン系レジメとしては, Paclitaxel (175～210 mg/m², 3週間隔, もしくは80 mg/m², 毎週連続投与) やDocetaxel 75 mg/m², 3週間隔の投与方法を中心に施行している. 38°C以上の熱発は比較的よく経験するものの, その多くはシプロキサンの内服で軽快している. 1日で解熱することが多いようであるが, その場合でも3日間内服は継続するように指導している. またこのような病態の場合, 次コース予定日(day22) には, 好中球は投与基準 (≧1,500/mm³) を満たしていることが多く, 次コース以降も減量せずに施行できている. 2コース目も同様の所見が観察されたときは, 減量も考慮する.

2003年5月から2005年10月にFEC療法を施行された165例を対象に, 検討した結果を引用する[12]. 165例中, 標準量として75 mg/m²で施行されたのは102例(以下FEC75), 90 mg/m²以上の高用量が施行されたのは63例(以下FEC100)であった. 完遂率は97.6%, Relative dose intensityは, FEC75群で0.94, FEC100群で0.92, 全体で0.93と良好である. 遅延や減量の理由として最も多いのは, 好中球の回復遅延であり, FEC75で19例 (18.6%), FEC100で16例 (25.4%), 計35例 (21.2%) に認められ, 高用量で頻度が高い. しかし, 発熱性好中球減少症 (シプロキサン® 無効例) で入院を要したのは, FEC75で2例 (2.0%), FEC100で4例 (6.3%), 計6例 (3.6%) のみであった. これらの症例は次コース目以降, 20～25%減量を行い, 予定クール数を完遂できている.

タキサン系の詳細なデータは未検討であるが, FEC療法に比べれば, 38°C以上の発熱の出現も比較的少ない印象があるが, 患者指導などは同様に十分留意している.

3) FN出現時の治療

シプロキサン® 無効の遷延性発熱, もしくは39°C以上の発熱による救急受診の際には, 検血 (白血球分画) とCRP, 胸部X線検査を行い, 好中球500/mm³未満で高度の炎症所見を認めた際には, 入院加療を勧める. 好中球が500/mm³以上の場合で発症より3日以内の場合は, シプロキサン® の内服で経過をみる. 当院の基本方針を図5に示す. 救急担当は他科のDrであることが多いために, 診断指針の基本はシェーマに示し, 救急外来に常備して, 統一を図っている.

入院治療の適応となった場合の, 初期治療は, セフェピム (マキシピーム®) 4 g/dayを2回分割投与とG-CSFを併用する. G-CSFは保険適応に従った用法用量で, 好中球5,000/mm³を目標にはするが, 速やかな解熱が認められたときは, その継続投与は中止する. 点滴抗生剤は, 3日間は最低継続する. 実際には好中球が100/mm³以下での入院の場合が多いが, 宿主の状態は良好であることが多く, 遷延化はまれである. 上記の6例中で, 1例のみマキシピーム® が無効で抗真菌薬で軽快した症例を経験した. 特に再発患者の場合は宿主の予備能力が小さいこともあり, FN時の病状悪化 (癌性リンパ管炎の悪化など) を引き起こす可能性も高く, 常に注意深い病状観察が必要である.

まとめ

発熱性好中球減少症に対する予防および治療方針に関して, ガイドラインを参考に, また乳癌化学療法における実際を当院の例をもとにまとめた. その多くは低リスク状態であることから, 適切な患者教育により, 外来通院による経口抗生物質で対応ができるが, ときにその無効例やGrade 4の好中球減少に高熱を伴う重症FNが発症することがある. 治療開始の遅延は致死的になりえる可能性があるため, 癌治療を行う病院では, 化学療法担当医のみならず, 病院全体として, 各スタッフがいつでも適格な診断と治療にあたれるような整備 (情報の共有) も重要である.

文　献

1) Masaoka T：Evidence-based recommendations for antimicrobial use in febrile neutropenia in Japan：Executive summary. *Clin Infect Dis* **39** (Suppl 1)：S49-52, 2004
2) Fever and neutropenia： treatment guidelines for patients with cancer. NCCN guideline, 2002
3) Klastersky J：The Multinational association for suppoetive care in cancer risk index：a multi national scoring system for identifying low-risk febrile neutropenic cancer patients. *J Clin Oncol* 18：3038-3051, 2000
4) Rolston KV：New trends in patient management：risk-based therapy for febrile patients with neutropenia. *Clin Infect Dis* **29**：515-521, 1999
5) Kanemaru A, Tatsumi Y：Microbiological data for patients with febrile neutropenia. *Clin Infect Dis* **39** (Suppl 1)：S8-11, 2004
6) Matsuhisa A, Saito Y, Ueyama H, et al：Detection of bacteria phagocytesmears from septicemia-suspected blood by in situ hybridization using biotinylated probes. *Microbiol Immunol* **38**： 511-517, 1994
7) Japanese translation of common terminology criteria for adverse events (CTCAE), and instructions and guidelines. *Int J Clin Oncol* **9** (Suppl 3)：1-82, 2004
8) Tamura K, Imajo K, Akiyama N, et al：Randomized trial of cefepime monotherapy or cefepime in combination with amikacin as empirical therapy for febrile neutropenia. *Clin Infect Dis* **39** (Suppl 1)：S16-25, 2004
9) Tamura K：Initial empirical antimicrobial therapy：duration and subsequent modifications. *Clin Infect Dis* **39** (Suppl 1)：S59-64, 2004
10) 日本癌治療学会臨床試験委員会編：G-CSF適正使用ガイドライン. 日癌治 **6** (別冊), 2001
11) Picazo J：Management of the febrile Neutropenic patient：a consensus conference. *Clin Infect Dis* **39** (Suppl 1)：S1-7, 2004
12) 増田慎三, 阿南節子, 石飛真人, 他：FEC療法におけるサポーティブケアの工夫. *Medical Oncologists* **1**(4)：55-62, 2005

Breast Cancer
Vol. 14 No. 1 January 2007

Case Report

Squamous Cell Carcinoma of the Breast in the Form of an Intracystic Tumor

Takashi Shigekawa*1,4, Hitoshi Tsuda*2, Kazuhiko Sato*1, Shigeto Ueda*1, Hideki Asakawa*1, Rena Shigenaga*1, Hoshio Hiraide*3, and Hidetaka Mochizuki*1

*Departments of *1Surgery I, and *2Pathology II, *3Research Institute, National Defense Medical College, *4Department of Breast Oncology, Saitama Medical University.*

Squamous cell carcinoma of the breast is thought to arise through metaplasia of ductal carcinoma cells. We report a case of pure squamous cell carcinoma of the breast with features of intracystic tumor, which was considered to have arisen from metaplastic squamous epithelial cells lining the cyst wall. A 71-year-old woman presented at our hospital with a 40×30-mm mass in the lower outer quadrant of the right breast. Mammography revealed a round, high-density mass, which had a mostly regular but partially irregular margin. Ultrasonography demonstrated a solid tumor with an irregular shape protruding into a cystic space, suspicious of intracystic carcinoma. Aspiration cytology confirmed squamous cell carcinoma. A modified radical mastectomy was performed. Histopathologically, the intracystic tumor was a pure squamous cell carcinoma. The epithelial cells lining the inner cyst wall showed mostly squamous metaplasia, and there was continuity between these cells and the squamous cell carcinoma. 13 months later, the patient is free of disease with no adjuvant therapy.

Breast Cancer 14:109-112, 2007.

Key words: Squamous cell carcinoma, Intracystic tumor

Introduction

Primary squamous cell carcinoma (SqCC) of the breast is a relatively uncommon disease, and is considered to arise through metaplastic change of ductal carcinoma cells. One clinicopathological finding that is characteristic of SqCC is a necrotic cystic space in the tumor center caused by rapid tumor growth. However, a few cases of SqCC occurring as an intracystic tumor have been reported. Here we report a case of primary SqCC of the breast in the form of an intracystic tumor, which was considered to have originated from epithelial cells with squamous metaplasia in the cyst wall.

Reprint requests to Takashi Shigekawa, Department of Breast Oncology, Saitama Medical University, School of Medicine. 38 Morohongo, Moroyama, Iruma-gun, Saitama 350-0495, Japan.
E-mail: t-shigekawa@h9.dion.ne.jp

Abbreviations:
SqCC, Squamous cell carcinoma; CIS, Carcinoma in situ

Received February 22, 2006; accepted October 4, 2006

Case Report

A 71-year-old post-menopausal woman was seen because of a right breast lump that had grown rapidly over several months. Physical examination revealed a well circumscribed and firm mass measuring 40×30-mm in the right inferior lateral quadrant. Nipple discharge was not evident, and there were no palpable axillary lymph nodes or supraclavicular nodes. She had no history of other carcinomas, including those of the oral cavity, esophagus, skin, uterus, vagina, or vulva. Mammography showed a round, high-density mass with an almost regular but partially irregular margin, measuring approximately 45×45- mm (Fig 1). Ultrasonography showed a circumscribed intracystic tumor measuring 39×33×31-mm. The nipple-tumor distance was 51-mm. The intracystic tumor was irregular in shape, had an indistinct margin, had continuity with the cyst wall, and was considered to be an intracystic carcinoma (Fig 2).

A fluid specimen obtained from the cystic lesion by fine-needle aspiration was not bloody,

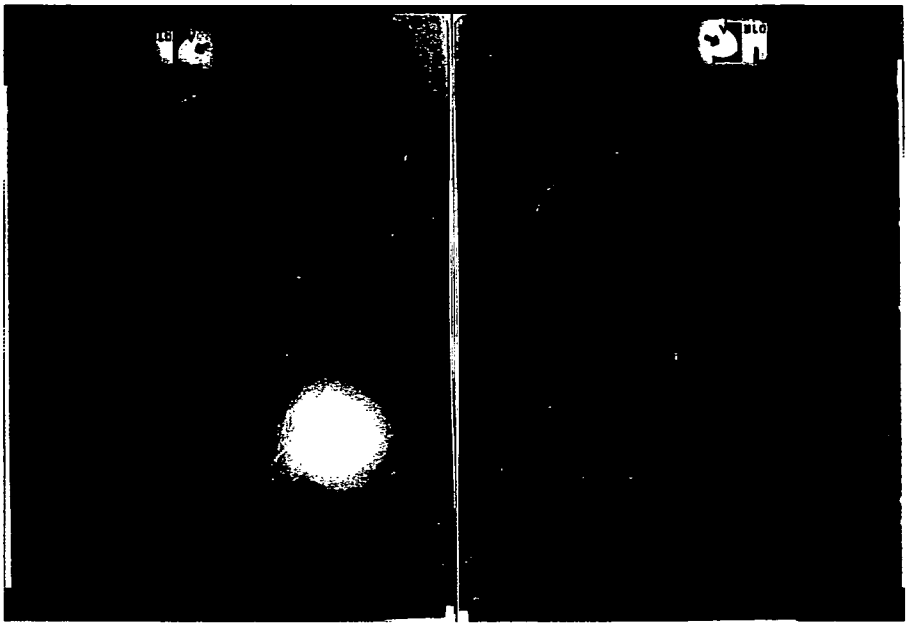

Fig 1. Mammography shows a round, high-density mass with an almost regular but partially irregular margin, measuring approximately 45 x 45 mm.

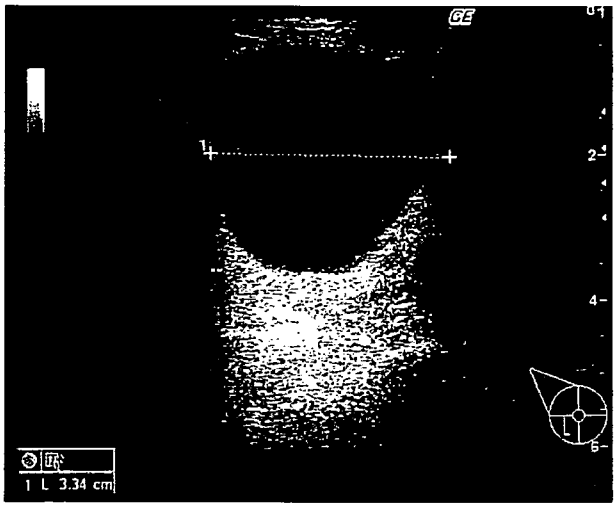

Fig 2. Ultrasonography shows a circumscribed intracystic tumor measuring 39 × 33 × 31-mm. The intracystic tumor was irregular in shape, had an indistinct margin, and was continuous with the cyst wall.

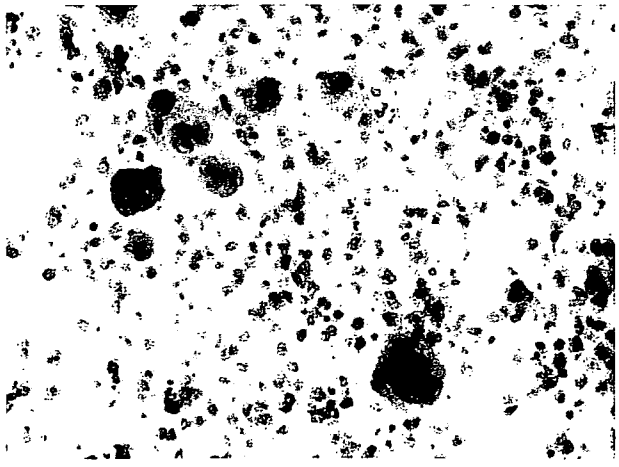

Fig 3. The cytopathological diagnosis of cells in the cystic fluid was malignancy consistent with SqCC. (Papanicolaou, magnification × 400)

but translucent and yellowish. Malignancy consistent with SqCC was diagnosed based on cytologic examination of cells in the cystic fluid. (Fig 3).

Laboratory data and tumor markers, including the levels of serum carcinoembryonic antigen, carbohydrate antigen 15-3, NCC-ST-439, and squamous cell carcinoma antigen were within the normal range. The preoperative staging of the tumor was T2N0M0, Stage II A.

A modified radical mastectomy with ipsilateral axillary lymph node dissection was performed. Macroscopically, the resected specimen revealed a grayish-white intracystic tumor measuring approximately 14 × 14 × 12-mm protruding into the cystic space, which measured approximately 47 x 25 x 34-mm (Fig 4).

Histopathologically, the tumor was intracystic, and it was composed of nests of atypical epithelial cells, showing stratification and cancer pearl formation (Fig 5a). The nuclei of the constituent tumor cells were irregular in size and shape, and showed hyperchromatism and a number of mitotic figures. There were no components of obvious invasive ductal carcinoma, non-invasive ductal car-

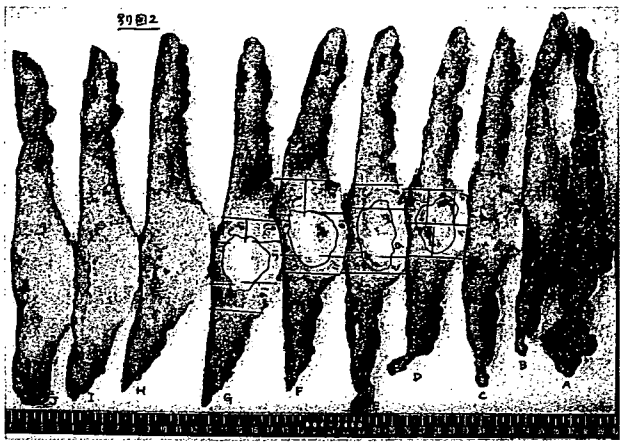

Fig 4. Macroscopically, the resected specimen reveals a grayish-white intracystic tumor measuring approximately 14 × 14 × 12-mm protruding into the cystic space, which measures approximately 47 × 25 × 34-mm.

cinoma, or other features of metaplastic carcinoma, for example spindle cells, or osseous or cartilaginous metaplasia. There was no continuity with adjacent cutaneous structures. Therefore, pure SqCC was diagnosed.

The tumor had invaded the cyst wall and adjacent adipose tissue of the breast. The cuboidal or flat epithelial cells lining the inner cyst wall had features of ductal epithelial origin, and sometimes showed squamous metaplasia (Fig 5b). There was continuity between the metaplastic epithelial cells and SqCC. Most of the cells lining the cyst wall were not normal epithelial cells but showed nuclear pleomorphism in shape and size, with relatively abundant and lightly eosinophilic cytoplasm (Fig 5c). Most of these cells were stratified into several layers, but sometimes occurred as a single layer. Therefore, these cells were believed to represent intraepithelial neoplasia or dysplasia arising from squamous metaplasia of the lining cells.

The SqCC cells were negative for estrogen and progesterone receptor, and the axillary lymph nodes were negative for metastasis.

No adjuvant therapy was performed. 13 months after the operation, the patient was asymptomatic and free of disease.

Discussion

SqCC of the breast is listed as a type of metaplastic carcinoma in the World Health Organization classification[1]. Toikkanen reviewed histopathological sections of about 4,000 diagnosed breast

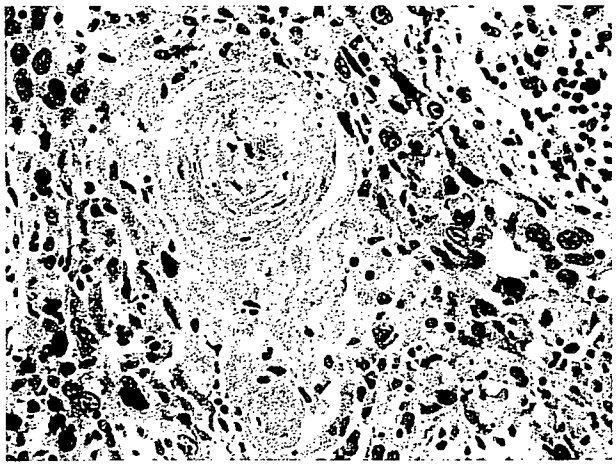

Fig 5a. : Histopathologically, the intracystic tumor is composed of nests of atypical epithelial cells, showing stratification and cancer pearl formation. The nuclei of the constituent tumor cells are irregular in size and shape, and shows hyperchromatism and a number of mitotic figures (Hematoxylin-Eosin, × 100).

Fig 5b. : The lining cells are thinly stratified and appear to show squamous metaplasia (Hematoxylin-Eosin, × 200).

Fig 5c. : Thickly stratified lining cells show nuclear pleomorphism in shape and size (Hematoxylin-Eosin, × 200).

carcinoma cases, and found only 3 cases (0.075%) of pure-type SqCC, and 20 cases (0.67%) of adenocarcinoma with squamous metaplasia, or mixed-type SqCC[2].

For a diagnosis of pure SqCC, Macia et al. stated that 3 conditions must be satisfied: (1) No other neoplastic components, such as ductal or mesenchymal elements, are present in the tumor; (2) The tumor is independent of adjacent cutaneous structures; (3) No other primary epidermoid tumors are present in the patient[3]. The present case satisfied all of these conditions. Additionally, the intracystic tumor was SqCC with no other neoplastic elements, and it had pathological continuity with the atypical squamous cells in the cyst wall. The epithelial cells lining the cyst wall were also atypical, accompanied mostly by features of squamous epithelium, but also with features of ductal epithelial cells. Therefore, this SqCC was considered to have arisen from duct epithelial cells in the cyst wall that showed squamous metaplasia, which later progressed to dysplasia or CIS.

The characteristics of SqCC of the breast generally reported are a large tumor size, rapid growth, and a single central cyst formed by necrosis[4,5]. In the present case, the tumor was large, 4.7 cm in diameter, and grew rapidly during a few months, but there was no single central cyst.

The most interesting characteristics of the present case were the features of the intracystic tumor and the continuity between the invasive SqCC and the atypical cells lining the cyst wall, suggesting that the SqCC originated from the wall of the cyst. There are several theories about the origin of SqCC of the breast. SqCC has been reported to originate from epidermal or dermoid cysts of the breast[6,7], chronic abscesses[7], skin[4], and complete metaplasia of glandular breast tissue.[8,9] It is likely that SqCC of the breast could arise through multiple histogenic pathways.

The treatment of pure SqCC does not differ from that of other common histological types of breast cancer and may involve surgery, chemotherapy, and irradiation therapy. As most cases of SqCC are negative for hormone receptors, hormonal therapy is not indicated[10]. However, because of its rarity, the most appropriate therapeutic regimens for SqCC are still unclear. Further reports are needed in order to acquire more information on possible therapeutic regimens for SqCC.

References

1) Tavassoli FA, Devilee P, Eds. World Health Organization Classification of Tumours. Pathology and Genetics of Tumours of the Breast and Female Genital Organs. IARC Press, Lyon, pp38-39, 2003.
2) Toikkanen S: Primary squamous cell carcinoma of the breast. *Cancer* 48: 1629-1632, 1981.
3) Macia M, Ces JA, Becerra E, Novo A: Pure squamous carcinoma of the breast; report of a case diagnosed by aspiration cytology. *Acta Cytol* 33: 201-204, 1989.
4) Cornog JL, Mobini J, Steiger E, Enterline HT: Squamous carcinoma of the breast. *Am J Clin Pathol* 55: 410-417, 1971.
5) Wargotz ES, Norris HJ: Metaplastic carcinoma of the breast. Squamous cell carcinoma of ductal origin. *Cancer* 65: 272-276, 1990.
6) Hasleton PS, Misch KA, Vasudev KS, George D: Squamous carcinoma of the breast. *J Clin Pathol* 31: 116-124, 1978.
7) Jones EL: Primary squamous-cell carcinoma of the breast with pseudosarcomatous stroma. *J Pathol* 97: 383-385, 1969.
8) Arffmann E, Hojgaard K: Squamous carcinoma of the breast: Report of a case. *J Pathol Bacteriol* 90: 319-321, 1965.
9) Soderstrom KO, Toikkanen S: Extensive squamous metaplasia simulating squamous cell carcinoma in benign breast papillomatosis. *Hum Pathol* 14: 1081-1082, 1983.
10) Woodard BH, Brinkhous AD, McCarty KS Jr, McCarty KS Jr: Adenosquamous differentiation in mammary carcinoma; an ultrastructural and steroid receptor study. *Arch Pathol Lab Med* 104: 130-133, 1980.

Reprinted with permission from the American Association for Cancer Research.

One-step Nucleic Acid Amplification for Intraoperative Detection of Lymph Node Metastasis in Breast Cancer Patients

Masahiko Tsujimoto,[1] Kadzuki Nakabayashi,[14] Katsuhide Yoshidome,[2] Tomoyo Kaneko,[8] Takuji Iwase,[9] Futoshi Akiyama,[8] Yo Kato,[8] Hitoshi Tsuda,[12] Shigeto Ueda,[13] Kazuhiko Sato,[13] Yasuhiro Tamaki,[3] Shinzaburo Noguchi,[3] Tatsuki R. Kataoka,[4] Hiromu Nakajima,[5] Yoshifumi Komoike,[6] Hideo Inaji,[6] Koichiro Tsugawa,[11] Koyu Suzuki,[10] Seigo Nakamura,[11] Motonari Daitoh,[14] Yasuhiro Otomo,[14] and Nariaki Matsuura[7]

Abstract **Purpose:** Detection of sentinel lymph node (SLN) metastasis in breast cancer patients has conventionally been determined by intraoperative histopathologic examination of frozen sections followed by definitive postoperative examination of permanent sections. The purpose of this study is to develop a more efficient method for intraoperative detection of lymph node metastasis.

Experimental Design: Cutoff values to distinguish macrometastasis, micrometastasis, and nonmetastasis were determined by measuring cytokeratin 19 (CK19) mRNA in histopathologically positive and negative lymph nodes using one-step nucleic acid amplification (OSNA). In an intraoperative clinical study involving six facilities, 325 lymph nodes (101 patients), including 81 SLNs, were divided into four blocks. Alternate blocks were used for the OSNA assay with CK19 mRNA, and the remaining blocks were used for H&E and CK19 immunohistochemistry–based three-level histopathologic examination. The results from the two methods were then compared.

Results: We established CK19 mRNA cutoff values of 2.5×10^2 and 5×10^3 copies/μL. In the clinical study, an overall concordance rate between the OSNA assay and the three-level histopathology was 98.2%. Similar results were obtained with 81 SLNs. The OSNA assay discriminated macrometastasis from micrometastasis. No false positive was observed in the OSNA assay of 144 histopathologically negative lymph nodes from pN0 patients, indicating an extremely low false positive for the OSNA assay.

Conclusion: The OSNA assay of half of a lymph node provided results similar to those of three-level histopathology. Clinical results indicate that the OSNA assay provides a useful intraoperative detection method of lymph node metastasis in breast cancer patients.

Sentinel lymph node (SLN) biopsy has recently become a standard surgical procedure in the treatment of breast cancer patients (1–10). This procedure can predict metastasis to the regional lymph nodes with high accuracy and avoids unnecessary removal of axillary lymph nodes and subsequent morbidity associated with axially clearance in node negative breast cancer patients.

SLN metastasis is generally detected by conventional means including the intraoperative H&E-based histopathologic examination of frozen section(s) or cytologic observation of touch-imprints, followed by definitive postoperative histopathologic examination of permanent sections (2, 7–9). However, the sensitivity of these intraoperative methods is not high. Many investigators have reported that the intraoperative H&E-based histopathologic examination has a false-negative rate of 5% to 52% (reviewed in ref. 11). Furthermore, these methods provide subjective rather than objective results, which may differ from one pathologist to another (12). On the other hand, the definitive postoperative histopathologic examination generally requires 5 to 10 days for assessment. If an accurate

Authors' Affiliations: Departments of [1]Pathology and [2]Surgery, Osaka Police Hospital, [3]Department of Breast and Endocrine Surgery, Osaka University Graduate School of Medicine, Departments of [4]Pathology, [5]Clinical Laboratory, and [6]Surgery, Osaka Medical Center for Cancer and Cardiovascular Diseases, and [7]Department of Molecular Pathology, Osaka University Graduate School of Medicine and Health Science, Osaka, Japan; Departments of [8]Pathology and [9]Breast Surgery, Cancer Institute of the Japanese Foundation for Cancer Research, and Departments of [10]Pathology and [11]Breast Surgical Oncology, St. Luke's International Hospital, Tokyo, Japan; Departments of [12]Pathology II and [13]Surgery I, National Defense Medical College, Saitama, Japan; and [14]Central Research Laboratories, Sysmex Corp., Kobe, Japan

Received 10/16/06; revised 4/3/07; accepted 5/15/07.

The costs of publication of this article were defrayed in part by the payment of page charges. This article must therefore be hereby marked *advertisement* in accordance with 18 U.S.C. Section 1734 solely to indicate this fact.

Note: Supplementary data for this article are available at Clinical Cancer Research Online (http://clincancerres.aacrjournals.org/).

M. Tsujimoto and K. Nakabayashi contributed equally to this work.

Requests for reprints: Nariaki Matsuura, Department of Molecular Pathology, Graduate School of Medicine and Health Science, Osaka University, 1-7 Yamadaoka, Suita, Osaka 565-0817, Japan. E-mail: matsuura@sahs.med.osaka-u.ac.jp.

© 2007 American Association for Cancer Research.

doi:10.1158/1078-0432.CCR-06-2512

intraoperative method is developed, the test results can allow for completion of axillary node dissection during surgery and avoidance of a second surgical procedure in patients with positive SLNs, thereby reducing patient distress and, finally, saving hospital costs (2, 13, 14). Accordingly, the development of a precise and objective intraoperative method for the detection of lymph node metastasis is important for increasing the efficiency of breast cancer surgery (10, 13-18).

To overcome the shortcomings of the present histopathologic methods, molecular biological methods based on quantitative reverse transcription-PCR (QRT-PCR) have been studied extensively for the detection of lymph node metastasis in breast cancer patients (12, 19-25). A QRT-PCR assay with multiple mRNA markers including cytokeratin 19 (CK19), trefoil factor 3 (p1B), epithelial glycoprotein 2 (EGP2), and small breast epithelial mucin (SBEM) resulted in a 10% upstaging compared with the routine histopathologic analysis (22). It was also reported that a QRT-PCR assay using mRNA markers of CK19 and mammaglobin 1 (MGB1) was almost as accurate (94.1% sensitivity and 98.6% specificity) as that of the conventional histopathologic examination (12). This study included a discussion of the drawbacks of using a single marker like CK19 mRNA for which the QRT-PCR may include the concomitant amplification of CK19 pseudogenes within genomic DNA, giving false positive results.

We recently developed a one-step nucleic acid amplification (OSNA) assay (Fig. 1A), which consists of solubilization of a lymph node followed by reverse-transcription loop-mediated isothermal amplification (RT-LAMP) of a target mRNA (26, 27). The RT-LAMP reaction is a new method of gene amplification, and its application has been reported previously (28-32). The OSNA method is characterized by the quantitative measurement of a target mRNA in a metastatic lymph node, a brief reaction time for the OSNA process, a high specificity for the target mRNA, and an absence of genomic DNA amplification.

In this paper, we report an efficient intraoperative detection method for lymph node metastasis in breast cancer patients using the OSNA assay with CK19 mRNA as a target marker. The results of a multicenter clinical study including 325 lymph nodes are discussed from the viewpoint of the usefulness of the OSNA assay as an intraoperative detection method.

Materials and Methods

Lymph nodes for selection of mRNA markers and determination of cutoff values. Lymph nodes, which were used to select mRNA markers and determine cutoff values, were obtained from Osaka Police Hospital with the approval of its internal review board. Lymph nodes were stored at -80°C until use.

QRT-PCR. QRT-PCR was carried out by ABI Prism 7700 sequence detector. RNA was purified from a lymph node lysate using RNeasy Mini Kit (Qiagen), and then purified RNA was subjected to one-step RT-PCR with QuantiTect SYBR Green (Qiagen) according to the manufacturer's instructions. The sequences of the forward and reverse primers used are shown in Supplementary Table S1. The primers were designed by Primer Express Version 2.0 software (ABI).

Selection of mRNA maker. Forty-five candidate mRNA markers, selected as being specific to breast cancer tissue, were identified from the public EST database (33). The performance of these mRNA markers was evaluated with QRT-PCR using a mixture of four histopathologically positive and four negative lymph nodes. The results were summarized as C_t (threshold cycle) values for each mRNA marker (see Supplementary Table S2). The selected markers, KRT19 (CK19), CEACAM5 (CEA), forkhead box A1 (FOXA1), SAM-pointed domain containing ETS transcription factor (SPDEF), tumor-associated calcium signal transducer 2 (TACSTD-2), mucin 1 (MUC1), and MGB1, were further evaluated with QRT-PCR using 11 histopathologically positive and 15 negative lymph nodes from 26 patients.

RT-LAMP reaction of CK19 mRNA. The RT-LAMP reaction was carried out according to the Notomi's method (26, 27). The human CK19 mRNA was synthesized by *in vitro* transcription from cloned cDNA.

A 2-μL sample of human CK19 mRNA in a lysis buffer containing 200 mmol/L glycine-HCl, 20% DMSO, and 5% Brij35 (pH 3.5) was added to 23 μL of solution consisting of 3.5 μmol/L each of the forward inner (CK19FA) and reverse primer (CK19RA), 0.2 μmol/L each of forward outer (CK19F3) and reverse primer (CK19R3), 2.6 μmol/L each of forward loop (CK19LPF) and reverse primer (CK19LPR), 0.9 mmol/L deoxynucleotide triphosphates, 54.3 mmol/L Tris-HCl, 10.8 mmol/L KCl, 10.8 mmol/L $(NH_4)_2SO_4$, 5.4 mmol/L $MgSO_4$, 0.1% Triton X-100, 5.4 mmol/L DTT, 2.5 units avian myeloblastosis virus reverse transcriptase (Promega), 18 units Bst DNA Polymerase (New England Biolabs), and 25 units RNasin Plus (Promega). Each reaction mixture contained three pairs of primer sets including the loop primer (27). The sequences of the human CK19 primers were designed as amplicons spanning exon junction regions between CK19 exons 1 and 2 and were

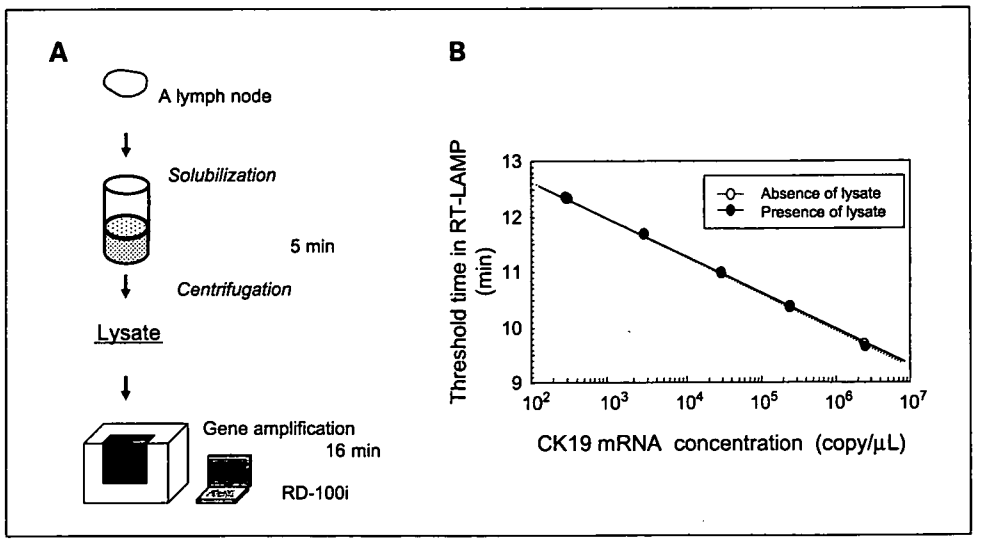

Fig. 1. OSNA assay. *A*, schematic diagram of the OSNA procedure. *B*, standard curve of human CK19 mRNA measured by RD-100i in the presence and absence of lymph node lysate. A histopathologically negative lymph node (600 mg) was homogenized in 4 mL of lysis buffer. A 180-μL sample of the lymph node lysate was added to 20 μL of human CK19 mRNA in the lysis buffer. The final concentration of human CK19 mRNA was adjusted to 2.5×10^6, 2.5×10^5, 2.5×10^4, 2.5×10^3, and 2.5×10^2 copies/μL. A 2-μL sample of each was subjected to the RT-LAMP reaction under the same conditions described in Materials and Methods.

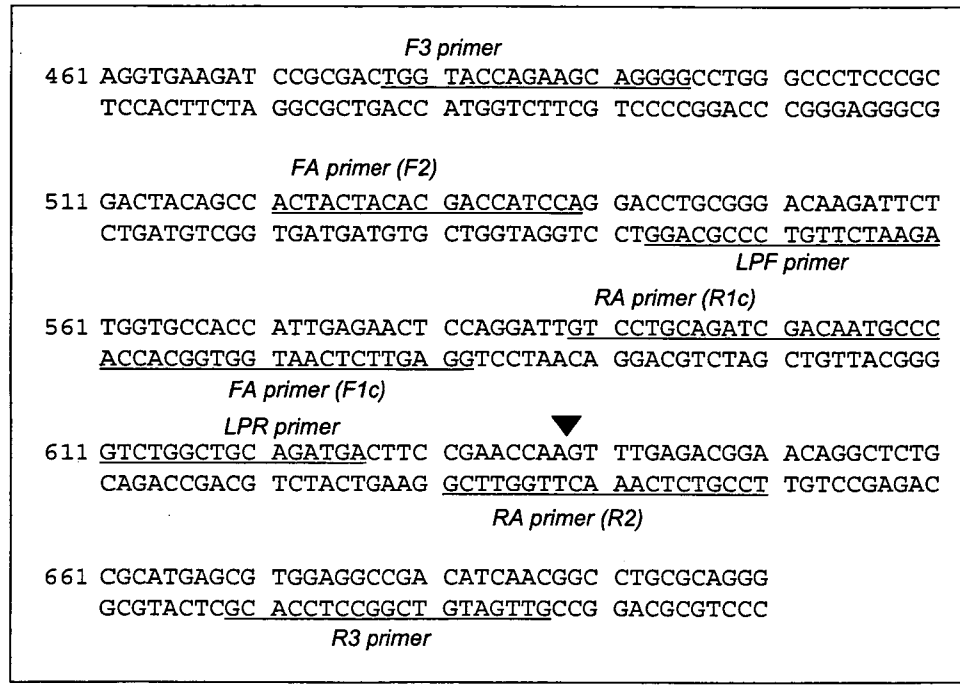

Fig. 2. A schematic representation of primer placement along the CK19 cDNA sequence. The CK19 cDNA sequence (NM.002276) and the sequence of the primers for the CK19 RT-LAMP are shown. The location on CK19 cDNA where each primer-set binds is underlined. The sequence of the inner primer (FA and RA) consists of discontinuous two different regions, F1c and F2 (or R1c and R2), to create the stem structure during the RT-LAMP reaction. The exon junction between exons 2 and 3 is included in the sequence of the R2 region in the RA primer (*arrowhead*).

furthermore designed as mismatch sequences of the CK19a and CK19b pseudogenes (GenBank accession number M33101 and U85961) using Probe Wizard (RNAture). Primer sequences were 5′-GGAGTTCT-CAATGGTGGCACCAACTACTACACGACCATCCA-3′ (CK19FA), 5′-GTCCTGCAGATCGACAACGCCTCCGTCTCAAACTTGGTTCG-3′ (CK19RA), 5′-TGGTACCAGAAGCAGGGG-3′ (CK19F3), 5′-GTTGATGTCGGCCTCCACG-3′ (CK19R3), 5′-AGAATCTTGTCCCG-CAGG-3′ (CK19LPF), and 5′-CGTCTGGCTGCAGATGA-3′ (CK19LPR). The sequence of each primer and its placement along the CK19 cDNA sequence are shown in Fig. 2.

The RT-LAMP reaction with CK19 mRNA was carried out in a gene amplification detector, RD-100i (Sysmex). Mori et al. (34, 35) reported that PPi, which is produced in the course of the RT-LAMP reaction, binds to magnesium ion to result in magnesium PPi. The amount of magnesium PPi increases with the passage of the reaction. Magnesium PPi has a low solubility in aqueous solution and precipitates when its concentration reaches saturation. The amplification of CK19 mRNA was monitored by measuring the turbidity of the reaction mixture at 6-s intervals. The threshold time was defined as the time at which the turbidity exceeded 0.1.

OSNA assay. A schematic diagram of the OSNA assay with CK19 mRNA is shown in Fig. 1A. A histopathologically negative lymph node (≤600 mg) was homogenized in 4 mL of the above lysis buffer for 90 s on ice using a Physicotron Warring blender with an NS-4 shaft (MicroTec Nichion). The homogenate was centrifuged at 10,000 × *g* for 1 min at room temperature. A 2-μL sample of the supernatant (lysate) was subjected to the RT-LAMP reaction under the same conditions as above. CK19 mRNA copy number was determined based on the standard curve using a known quantity of human CK19 mRNA.

Effect of lymph node size on the OSNA assay. A histopathologically negative lymph node (130 mg) was homogenized in 4 mL of lysis buffer under the same conditions as above. A 180-μL sample of lymph node lysate was added to 20 μL of human CK19 mRNA in the lysis buffer. The final concentration of human CK19 mRNA was adjusted to 2.5×10^5 and 2.5×10^3 copies/μL. About 2 μL of each sample was subjected to the RT-LAMP reaction under the same conditions described above. Each sample was assayed in duplicate. Other histopathologically negative lymph nodes (214, 354, and 428 mg) were treated under the same conditions as above.

Amplification of genomic DNA by the OSNA assay. Genomic DNA was extracted from histopathologically positive lymph nodes using QIAamp DNA Mini Kit (Qiagen) according to the manufacturer's instructions. Purified genomic DNA (100 ng) was subjected to the OSNA assay using the CK19 primers described above.

Protocol for determining the cutoff values. A cutoff value (*L*) for the OSNA assay between metastatic positive and negative lymph nodes was determined using 106 lymph nodes (42 histopathologically negative lymph nodes from pN0 patients, 42 histopathologically negative lymph nodes from pN1-3 patients, and 22 histopathologically positive lymph nodes) from 30 patients (24 ductal carcinomas, 5 special types, and 1 ductal carcinoma *in situ*). As shown in Fig. 3A, the central part of one quarter of a frozen lymph node (40-600 mg) of 1 mm thickness was dissected out. Four levels (i, ii, iii, and iv) were used as permanent slices for the histopathologic examination with H&E and immunohistochemistry using anti-CK19 antibody (DAKO) as shown in Fig. 3A.

Histopathologically positive lymph nodes were defined as those that were positive at any of four levels (i, ii, iii, and iv). Histopathologically negative lymph nodes were defined as those that were negative in all four levels. Blocks a and c were used for the OSNA assay. A cutoff value was determined by statistical analysis of the copy numbers obtained by the OSNA assay of the histopathologically negative lymph nodes from pN0 patients.

According to the tumor-node-metastasis (TNM) classification of the Unio Internationale Contra Cancrum (Italian) sixth and the American Joint Committee on Cancer sixth editions (36), macrometastasis is defined as having metastatic foci of ≥2 mm in the long axis. In the OSNA assay, macrometastasis is assumed as having the amount of CK19 mRNA expression in 2^3 mm^3 of metastatic foci. Based on this assumption, we estimated a cutoff value (*H*) for CK19 mRNA between macrometastasis and micrometastasis as follows. Nine frozen histopathologically positive lymph nodes from nine breast cancer patients (8 ductal and 1 lobular carcinomas) were used to estimate the amount of CK19 mRNA expression in 2^3 mm^3 of metastatic foci (Table 1). A frozen lymph node was serially sectioned at 10-μm intervals. Each slice was first examined with CK19 immunohistochemistry-based histopathologic examination to measure the area of metastatic foci and then with RT-LAMP to measure CK19 mRNA expression. The procedure is detailed in Fig. 3B.

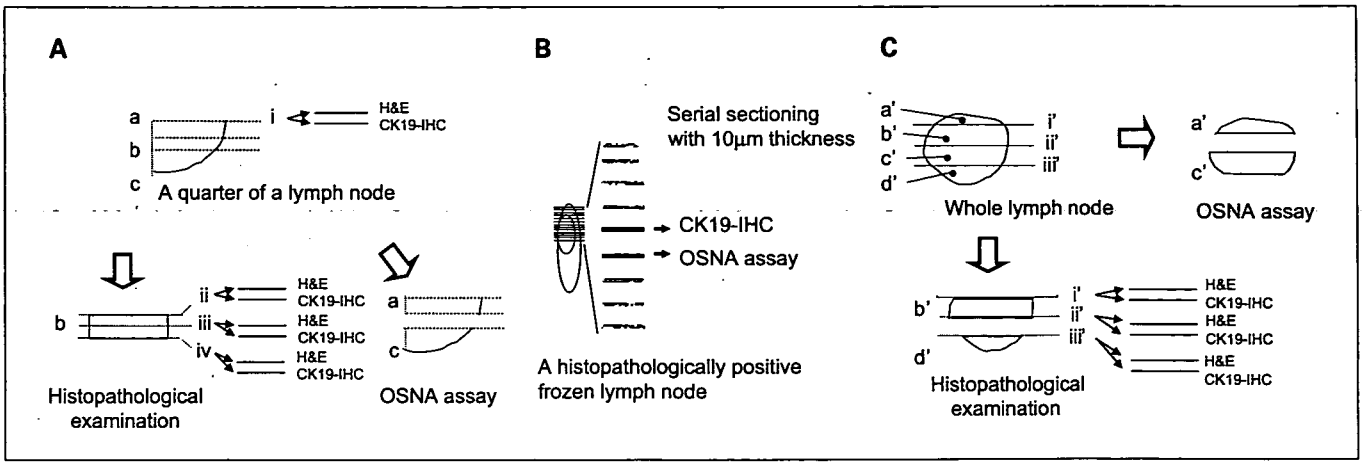

Fig. 3. Protocols. *A*, protocol for determining a cutoff value for micrometastasis and nonmetastasis. *B*, protocol for determining the cutoff value between macrometastasis and micrometastasis. Serial frozen sections taken at 10-μm intervals were prepared from histopathologically positive lymph nodes. One of two consecutive frozen sections was subjected to CK19 immunohistochemistry (CK19-IHC) – based histopathologic examination to measure the area of metastatic foci, and then the volume of the metastatic foci was calculated by multiplying the area by the thickness of the slice. The adjacent section was subjected to the OSNA assay. The expression level of CK19 mRNA in 2^3 mm^3 was estimated based on the correlation between the volume of metastatic foci and CK19 mRNA expression. *C*, clinical study protocol.

In the OSNA assay, an amount of CK19 mRNA expression less than the cutoff value was indicated as (-), an amount of CK19 mRNA expression between the cutoff values *L* and *H* was indicated as (+), and an amount of CK19 mRNA expression greater than the cutoff value *H* was indicated as (++).

Clinical study protocol. An intraoperative clinical study was conducted from February 2005 to July 2005 at six facilities other than Sysmex Central Research Laboratories. A total of 325 fresh lymph nodes (101 patients), including 81 SLNs (49 patients), were used with the approval of the internal review board at each facility. The clinicopathologic characteristics of patients are shown in Table 2. A large percent of patients had stages I A/B and II A/B. The majority of patients had a nodal status of pN0 and pN1. About 80% of patients had invasive ductal carcinoma.

A fresh lymph node with a short axis of 4 to 12 mm was divided into four blocks at 1- or 2-mm intervals using our original cutting device (Fig. 3C and 4). Blocks a′ and c′ were used for the OSNA assay. Two slices were cut from each of the three cutting surfaces (i′, ii′, and iii′), as shown in Fig. 3C, and used for the permanent three-level histopathologic examination with H&E and CK19 immunohistochemistry.

In the histopathologic examination, macrometastasis and micrometastasis were defined according to the TNM classification of the Unio Internationale Contra Cancrum sixth and American Joint Committee on Cancer sixth editions (36). All samples for histopathologic examination were examined by three third-party pathologists. Conflicting results were settled consensually. The performance of the OSNA assay was compared with the three-level histopathology.

The OSNA assay analyzed different blocks from those used in the three-level histopathologic examination. Therefore, in this protocol, the sensitivity and specificity of the OSNA assay could not be calculated based on the histopathologic results. For this reason, we evaluated the performance of the OSNA assay as a concordance rate with the three-level histopathologic examination.

In the case of lymph nodes from pN0 patients, blocks b′ and d′ were further sliced at 0.2-mm intervals, followed by staining each alternate slice with H&E and CK19 immunohistochemistry (Fig. 3C). A total of 144 lymph nodes, in which neither macrometastasis nor micrometastasis were observed in the above serial sectioning examination, were used for the false positive study of the OSNA assay.

When discordance between the OSNA assay and the three-level histopathologic examination occurred, a histopathologic analysis of blocks b′ and d′ was repeated. All slides for the histopathologic examination were examined and evaluated by three third-party pathologists. All results of histopathologic examinations were finally determined by a study group comprised of representatives from the different facilities.

Analysis of discordant cases. In the analysis of discordant cases, QRT-PCR and CK19 Western blot analysis of the lysates were carried out. QRT-PCR was carried out with TaqMan RT-PCR. RNA was purified from lymph node lysates using RNeasy Mini Kit (Qiagen), and then the purified RNA was subjected to TaqMan one-step RT-PCR universal master mix (ABI) according to the manufacturer's instructions. The sequences of the forward and reverse primers designed for human CK19 were 5′-CAGATCGAAGGCCTGAAGGA-3′ and 5′-CTTGGCCCCT-CAGCGTACT-3′, respectively. The sequence of the TaqMan probe, containing a fluorescent reporter dye (FAM) at the 5′ end and a fluorescent quencher dye (TAMRA) at the 3′ end, was 5′-FAM-GCCTACCTGAA-GAAGAACCATGAGGAGGAA-TAMRA-3′. The primers and TaqMan probe were obtained from Applied Biosystems (ABI). All QRT-PCR reactions were done in duplicate.

In the CK19 Western blot analysis, lysate (20 μL) was added to 10 μL of loading buffer containing 150 mmol/L Tris-HCl, 300 mmol/L DTT, 6% SDS, 0.3% bromophenol blue, and 30% glycerol. The solution was boiled and electrophoresed on a polyacrylamide gel in the presence of

Table 1. CK19 mRNA expression in 2^3 mm^3 of metastatic foci

Case	Histology	CK19 mRNA (copy/μL)
1	Ductal carcinoma	2.3×10^4
2	Ductal carcinoma	1.1×10^4
3	Ductal carcinoma	4.7×10^3
4	Ductal carcinoma	5.0×10^4
5	Ductal carcinoma	1.0×10^4
6	Lobular carcinoma	1.4×10^5
7	Ductal carcinoma	2.0×10^4
8	Ductal carcinoma	6.7×10^4
9	Ductal carcinoma	2.4×10^4
	Average	3.0×10^4

NOTE: CK19 mRNA expression in 2^3 mm^3 of metastatic foci was estimated on the basis of the examination of serial sections (Fig. 3B).

Table 2. Clinicopathologic characteristics of patients

	Number of patients
Stage	
0	5
I A/B	41
II A/B	49
III A/B/C	5
IV	1
Nodal status	
pN0	60
pN1	35
pN2	2
pN3	4
Histopathologic type	
Invasive ductal carcinoma	87
Neuroendocrine carcinoma	1
Matrix producing carcinoma	1
Mucinous carcinoma	2
Apocrine carcinoma	1
Invasive lobular carcinoma	4
Ductal carcinoma *in situ*	5

SDS (PAG Mini; Daiichi Pure Chemicals). After electrotransfer to Immobilon-FL polyvinylidene difluoride membranes (Millipore), the membrane was blocked with skim milk (BD Bioscience) for 1 h at room temperature. The primary antibody, anti-CK19 (A53-B/A2; Santa Cruz Biotechnology), was diluted 1:500 with TBS-Tween 20 (TBS-T) solution, and the membrane was incubated at 4°C overnight with anti-CK19 antibody. The membrane was then washed with TBS-T and incubated with a secondary antibody conjugated with horseradish peroxidase, which was diluted 1:2,000 with TBS-T. After washing the membrane twice with TBS-T, CK19-CK19 antibody complex was visualized using the ECL-Advance detection kit (GE Healthcare). The intensity of the signal in each band was evaluated by LumiAnalyst (Roche). CK19 protein concentration was determined based on a standard curve that was obtained by measuring known quantities of CK19 protein (Biodesign) of 0.15, 0.075, 0.038, and 0.018 ng/μL.

A cutoff value for CK19 protein expression between histopathologically positive and negative lymph nodes was determined by Western blot analysis of 37 histopathologically negative lymph nodes from 16 pN0 patients, 54 histopathologically negative lymph nodes from 17 pN1-3 patients, and 22 histopathologically positive lymph nodes from 12 patients (Figs. 3A and 5A). The cutoff value was determined by statistical analysis of the amount of CK19 measured by Western blot analysis of 37 histopathologically negative lymph nodes from 16 pN0 patients.

Results

Selection of the mRNA marker. We evaluated mRNAs for CK19, CEA, FOXA1, SPDEF, MUC1, and MGB1 using 11 histopathologically positive and 15 negative lymph nodes from 26 patients. The absolute mRNA expression levels of CEA and MGB1 in metastatic lymph nodes were not as high as expected, whereas the absolute expression levels of MUC1 mRNA in nonmetastatic lymph nodes was relatively high. For these reasons, CEA, MGB1, and MUC1 mRNAs were not selected for the OSNA assay.

The expression levels of CK19, FOXA1, and SPDEF mRNAs differed between histopathologically positive and negative lymph nodes. However, the lower limits of the expression levels of FOXA1 and SPDEF mRNAs in histopathologically positive lymph nodes were 4 to 30 times less than that of CK19 mRNA (Fig. 6). On the other hand, the detection limit of the OSNA assay was nearly equivalent to 32 threshold cycles of the RT-PCR system. An assay system should detect the upper limit of the expression levels of an mRNA marker in histopathologically negative lymph nodes. The upper limits of the threshold cycle of FOXA1 and SPDEF mRNAs were about 35 and 32,

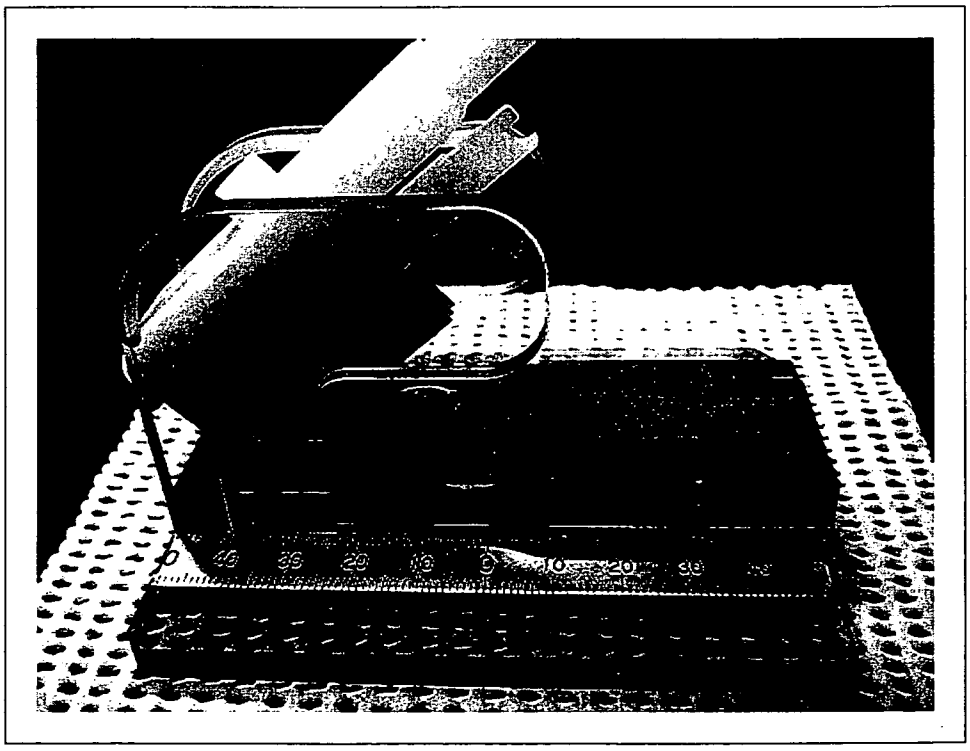

Fig. 4. Lymph node cutting device.

respectively. For these reasons, we determined CK19 mRNA to be the best marker for the OSNA assay.

OSNA assay. As shown in Fig. 1B, an inverse correlation between the threshold time in the RT-LAMP step and CK19 mRNA concentration was observed in a range of CK19 mRNA concentrations of 2.5×10^2 to 2.5×10^6 copies/μL, and both curves overlapped completely in the presence and absence of the lymph node lysate; the correlation coefficient value in both cases was 0.99. This result indicates that factors that may be present in lymph node lysates do not interfere with the OSNA assay.

Effect of lymph node size on the OSNA assay. The threshold time of the OSNA assay with 2.5×10^3 and 2.5×10^5 copies/μL of CK19 mRNA in a lysate obtained from 130 mg of lymph node was 10.9 and 9.6 min, respectively. The threshold time with 2.5×10^3 copies/μL of CK19 mRNA in a lysate obtained from a lymph node of 214, 354, and 428 mg was 10.7, 10.9, and 10.9 min, respectively, whereas the time with 2.5×10^5 copies/μL of CK19 mRNA in a lysate obtained from a lymph node of 214, 354, and 428 mg was 9.6, 9.7, and 9.7 min, respectively. The threshold times with 2.5×10^3 and 2.5×10^5 copies/μL of human CK19 mRNA in the lysates obtained from lymph nodes of 130, 214, 354, and 428 mg were within an acceptable error range. The results indicate that the OSNA assay is not influenced by lymph node size.

Amplification of genomic DNA by the OSNA assay. To exclude the possibility of genomic DNA amplification in the OSNA assay, we examined the OSNA assay using genomic DNA purified from lymph nodes. Genomic DNA was not amplified from either metastatic or nonmetastatic lymph nodes. The results indicate that the OSNA assay amplifies only CK19 mRNA.

Cutoff values. A cutoff value for the OSNA assay between histopathologically positive and negative lymph nodes was determined by the logarithmic normal distribution of CK19 mRNA copy numbers from 42 lymph nodes from pN0 patients. The average value of CK19 mRNA expression +3 SD was 2.5×10^2 copies/μL. Based on this analysis, we set the cutoff value at 2.5×10^2 copies/μL, which represents the upper limit of the copy numbers in the histopathologically negative lymph nodes from pN0 patients (Fig. 7A).

To validate the cutoff value, we examined CK19 mRNA expression in 42 histopathologically negative lymph nodes from 16 pN1-3 patients. Only one of these 42 cases showed $>2.5 \times 10^2$ copies/μL CK19 mRNA (Fig. 7B). This lymph node showed 3×10^3 copies/μL of CK19 mRNA. This suggested that micrometastatic foci in block a or c (Fig. 3A) of the lymph node were included in the sample. On the other hand, CK19 mRNA expression in all 24 pathologically positive lymph nodes from 10 patients exceeded the cutoff value (Fig. 7C).

To obtain a cutoff value for CK19 mRNA expression between macrometastasis with metastatic foci $>2^3$ mm^3 and micrometastasis, we compared CK19 mRNA expression in serial sections of a lymph node with an area of metastatic foci and roughly estimated macrometastasis to be $>5 \times 10^3$ copies/μL, which is the lowest value of CK19 mRNA expression found in metastatic foci of 2^3 mm^3 (Table 1).

Accordingly, for the OSNA assay, we defined macrometastasis (++) as $>5 \times 10^3$ copies/μL of CK19 mRNA, micrometastasis (+) as 2.5×10^2 to 5×10^3 copies/μL, and nonmetastasis (-) as $<2.5 \times 10^2$ copies/μL.

Clinical study. All OSNA assays were carried out during surgery and were completed within 30 min. H&E and CK19 immunohistochemistry were used in the histopathologic examination.

Isolated tumor cells (ITC) are widely used as one of indicators in a nomogram-aiding treatment decisions. In the American Society of Clinical Oncology guidelines (10), ITCs are described as having unknown clinical significance, and there are insufficient data to recommend appropriate treatment, including axillary lymph node dissection. For this reason, we viewed ITC as negative.

Table 3 shows the results of CK19 immunohistochemistry in all samples with the H&E results given in parenthesis. H&E-based histopathology failed to detect 1 of 40 cases of macrometastasis and 3 of 5 cases of micrometastasis. Overall, the sensitivity of H&E-based histopathology was 91.1% based on the results of CK19 immunohistochemistry–based histopathology. The sensitivities of the one- and two-level CK19

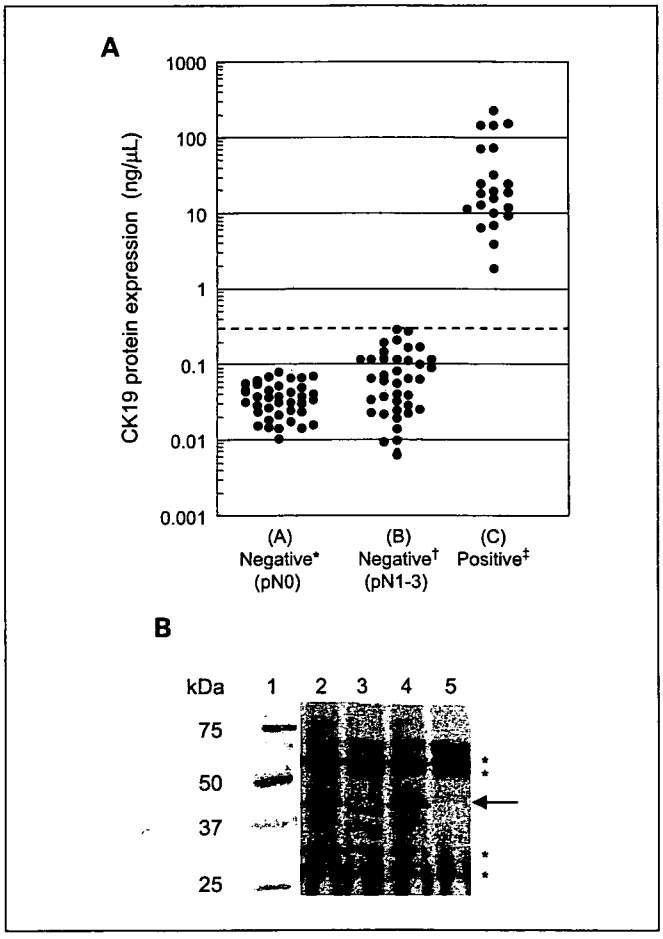

Fig. 5. CK19 protein expression in lymph node lysates. *A*, CK19 protein expression in histopathologically positive and negative lymph node lysates. *, histopathologically negative lymph nodes dissected from pN0 patients. †, histopathologically negative lymph nodes dissected from pN1-3 patients. ‡, histopathologically positive lymph nodes. The CK19 protein expression was determined by Western blot analysis (see Materials and Methods). Broken line, cutoff line between micrometastasis and nonmetastasis. The protein concentration of representative lymph node lysates used in this experiment was within the range of 8.7 to 11.6 μg/μL. *B*, a representative example of Western blot analysis of CK19 protein in lymph node lysates. Lane 1, molecular weight markers stained with Coomassie brilliant blue. Lanes 2 and 4, histopathologically positive lymph node lysate. Lanes 3 and 5, histopathologically negative lymph node lysate. Arrow, CK19 protein. *, nonspecific bands. The vertical scale shows molecular weights.

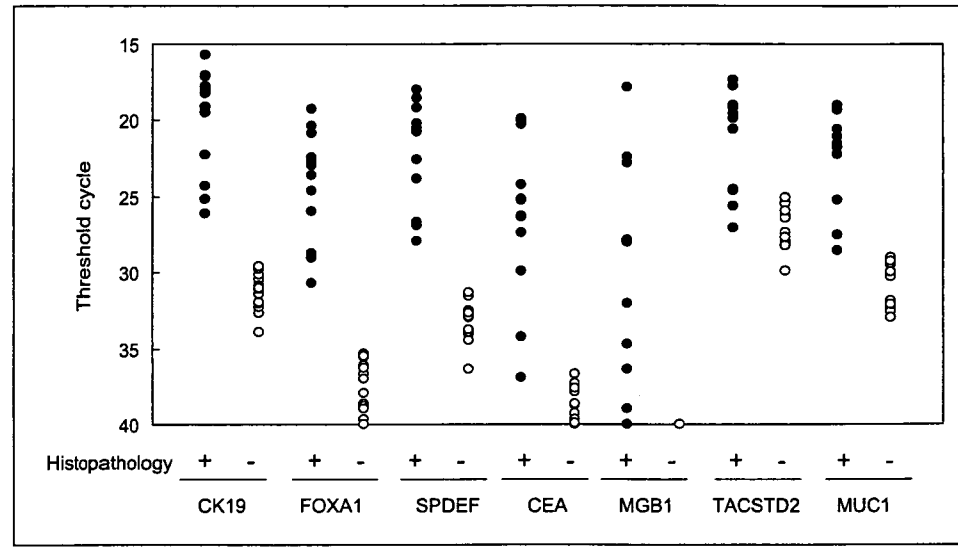

Fig. 6. Expression of mRNA markers in histopathologically positive and negative lymph nodes. The selected mRNA markers (CK19, FOXA1, SPDEF, CEA, MGB1, TACSTD2, and MUC1) were evaluated by QRT-PCR using 11 histopathologically positive (●) and 15 negative (O) lymph nodes from 26 patients.

immunohistochemistry-based histopathologies were 86.7% and 91.1%, respectively, based on the results of three-level CK19 immunohistochemistry-based histopathology (Supplementary Table S3).

The concordance rate between the OSNA assay and the CK19 immunohistochemistry-based three-level histopathology for 325 lymph nodes was 98.2%. The concordance rate for SLNs was 96.4%.

No false positive results were found with the OSNA assay of 144 histopathologically negative lymph nodes from 60 pN0 patients, in which neither micrometastasis nor macrometastasis was observed for serial sections from blocks b′ and d′ (Fig. 3C). Furthermore, the OSNA assay judged 13 ITC cases as negative. These results are summarized in Table 3.

Discordant cases. Six discordant cases were observed between the OSNA assay and CK19 immunohistochemistry-based histopathologic examination (Table 4). Four cases were micrometastasis according to the OSNA assay and were negative according to the CK19 immunohistochemistry-based histopathology. In any case, CK19 mRNA expression of $>10^3$ copies/μL was observed (Table 4). These four discordant cases came from pN1 and pN2 patients. In two of four cases, micrometastasis was observed in the multilevel examinations of blocks b′ and d′. On the other hand, two remaining cases (Table 4, *samples 5* and *6*) were negative according to the OSNA assay and micrometastasis according to the three-level histopathology. Samples 5 and 6 showed metastatic foci of 0.3 and 0.4 mm in the long axis, which were observed on surfaces i′ and ii′, respectively. When i′ and ii′ were histopathologically examined, about 0.2 mm was shaved from the surfaces of blocks b′ and d′. Therefore, the amount of metastatic foci in blocks a′ and c′ that were used for the OSNA assay (i.e., a′ and c′) could not be quantified.

We also measured the amount of CK19 protein by Western blot analysis of the lysate used in each discordance case. A cutoff value for CK19 protein expression between metastasis positive and negative lymph node was determined by the distribution of CK19 protein expression in 37 histopathologically negative lymph nodes from 16 pN0 patients. The distribution could be described as a logarithmic normal distribution. The statistical analysis indicated that an average value +3 SD was 0.13 ng/μL. Based on this analysis, the cutoff value was determined to be 0.3 ng/μL, which is the upper limit of the CK19 protein expression in 54 histopathologically negative lymph nodes from pN1-3 patients (Fig. 5A). Furthermore, CK19 protein expression in 22 histopathologically positive lymph nodes from 10 patients contained protein levels over the cutoff value.

Based on this cutoff value, we measured the amount of CK19 protein using quantitative Western blot analysis of the lysate for the OSNA assay of samples 1, 2, and 5. As described in Table 4, samples 1 and 2 showed an amount of CK19 protein expression equivalent to micrometastasis. Sample 5 exhibited no CK19 protein expression.

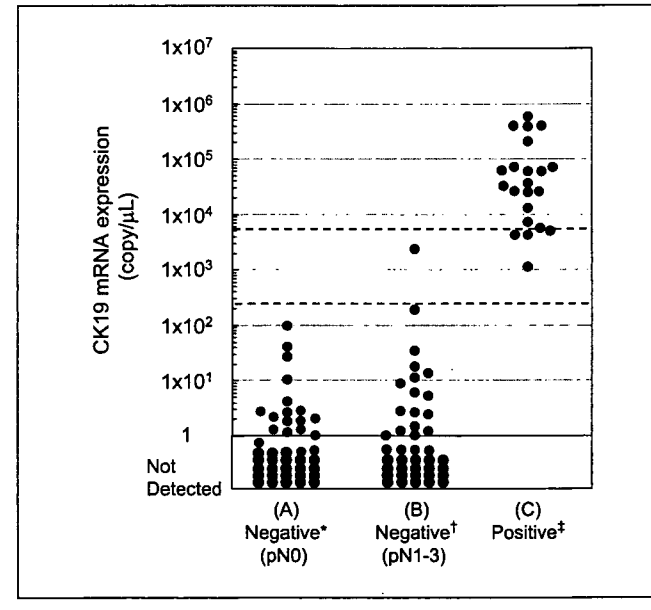

Fig. 7. CK19 mRNA expression in the OSNA assay carried out under the protocol A (Fig. 3 A). *, histopathologically negative lymph nodes dissected from pN0 patients. †, histopathologically negative lymph nodes dissected from pN1-3 patients. ‡, histopathologically positive lymph nodes. Top broken line, cutoff between macrometastasis and micrometastasis. Bottom broken line, cutoff between micrometastasis and nonmetastasis.